

Reading Single DNA with DNA Polymerase Followed by Atomic Force Microscopy

Youngkyu Kim,[†] Eung-Sam Kim,^{†,‡} Yoonhee Lee,[‡] Jung-Hun Kim,^{†,§} Bong Chu Shim,^{||} Seong Moon Cho,^{||} Jeong Soo Lee,^{||} and Joon Won Park^{*,†,‡}

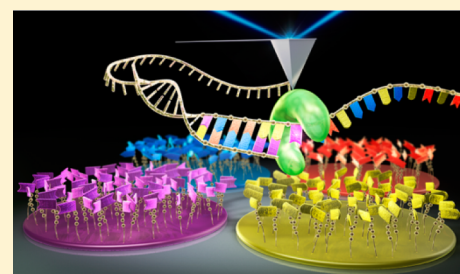
[†]School of Interdisciplinary Bioscience and Bioengineering, [‡]Department of Chemistry, and [§]Department of Life Sciences, Pohang University of Science and Technology, San 31 Hyoja-dong, Pohang, 790-784, Korea

^{||}Materials & Components Laboratory, LG Electronics Advanced Research Institute, 38 Baumoe-ro, Seocho-gu, Seoul, 137-724, Korea

[‡]Department of Biological Sciences, Chonnam National University, 77 Yongbong-ro, Buk-gu, Gwangju, 500-757, Korea

Supporting Information

ABSTRACT: The importance of DNA sequencing in the life sciences and personalized medicine is continually increasing. Single-molecule sequencing methods have been developed to analyze DNA directly without the need for amplification. Here, we present a new approach to sequencing single DNA molecules using atomic force microscopy (AFM). In our approach, four surface-conjugated nucleotides were examined sequentially with a DNA polymerase-immobilized AFM tip. By observing the specific rupture events upon examination of a matching nucleotide, we could determine the template base bound in the polymerase's active site. The subsequent incorporation of the complementary base in solution enabled the next base to be read. Additionally, we observed that the DNA polymerase could incorporate the surface-conjugated dGTP when the applied force was controlled by employing the force-clamp mode.



the applied force was controlled by employing the force-clamp mode.

INTRODUCTION

DNA carries the crucial information on living systems via four bases, and DNA base mutations can cause diseases and modified responses to drugs.¹ Thus, efficient DNA sequencing promises personalized diagnosis and treatment, and so-called next-generation technologies have been developed for rapid and affordable sequencing.^{2,3} These technologies are based on massively parallel analysis of fragmented DNA using enzymatic reactions coupled with optical detection. Recently, the use of ion-sensitive field effect transistors for detection was reported.⁴ These tools have enabled rapid sequencing with high throughput but require amplification steps that may generate sequencing artifacts.

As an alternative to current next-generation technologies, single-molecule sequencing methods have received much attention from academia and industry.⁵ These methods can be classified into two categories: sequencing-by-synthesis (SBS) and direct sequencing. For SBS, sequencing at the intrinsic speed of a DNA polymerase (DNAP) has been realized by monitoring the fluorescence of incorporated bases or the base-specific conductance change of the DNAP.^{6,7} Most direct sequencing methods exploit electrical measurements. With the use of membrane-embedded or solid-state nanopores, base-specific current blockage is measured as a DNA molecule passes through the pore.^{8,9} Scanning tunnelling microscopy was used to recognize guanines along an extended single-stranded DNA and to discriminate cytosine from adenine in an oligonucleotide using a functionalized probe.^{10,11} Both approaches boast the

advantages of faster sequencing with a minute amount of sample and of not requiring amplification steps. However, low signal-to-noise ratio, signal overlap among the four DNA bases, and photobleaching are issues with these methods that must be addressed. Recently, reports have indicated that force manipulation tools, such as optical tweezers and magnetic tweezers, may be able to address these difficulties.^{12,13}

AFM is a force manipulation tool that has been used to observe molecular interactions at the single-molecule level, manipulate single molecules, and map the distribution of biomolecules at the nanometer resolution.^{14–20} There have been several attempts to use AFM as a sequencing tool. In 1991, AFM-based sequencing was suggested, but the resolution of this method was not high enough to discern each base.²¹ Therefore, an indirect method of using streptavidin- or fluorophore-labeled complementary oligonucleotides was proposed, and the presence and location of target sequences could be observed in the AFM image.²² More recently, a molecular ring was devised to move along a single-stranded DNA, and the friction force on the ring was measured. However, discriminating bases according to the differences in friction force was not possible with the employed pulling speed of AFM.²³ Recently, tip-enhanced Raman spectroscopy was used to sequence a single RNA cytosine homopolymer.²⁴

Received: June 25, 2014

Published: September 9, 2014

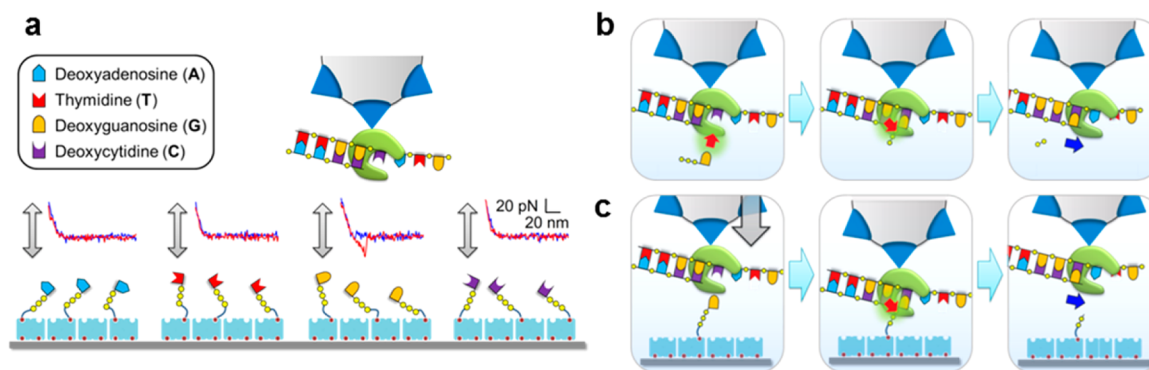


Figure 1. Force-based DNA sequencing using AFM. In this schematic, the base in the active site of the DNAP on the AFM tip is cytosine. (a) Schematic of the recognition step. When the DNAP on the AFM tip (blue cones represent the dendron molecules, which coat the AFM tip) captures a primer-template DNA, retraction of the AFM tip results in a rupture curve. When the approach/retraction of the tip is repeated on four dNTP spots, specific rupture curves are expected to be predominantly observed on the matching dNTP (dGTP) spot. The force–distance curves in this schematic are from the experimental data. (b) Schematic of in-solution incorporation. When the AFM tip is immersed in a dGTP solution, a dGTP will fit in the active site of the DNAP/DNA and will be incorporated at the 3'-end of the primer. (c) Schematic of on-chip incorporation. When the AFM tip is brought to a dGTP that is immobilized on the surface and kept in contact for a certain time, that dGTP can be incorporated into the primer. In both cases, the DNAP on the AFM tip is ready to recognize the next complementary base after incorporation.

Here, we present a new DNA sequencing method based on AFM force spectroscopy. The specific base bound in the active site of a DNAP can be recognized by AFM. The recognized base is then incorporated into the primer by dipping the AFM tip into a solution of the corresponding deoxyribonucleoside triphosphate (dNTP), and the two-step process is repeated to read the sequence. The incorporation of dNTPs immobilized on surfaces was also investigated, and the incorporation of dGTP with an intriguing dependence of DNAP activity on the applied force was observed.

RESULTS

Recognition and Incorporation as the Key Steps. We designed a DNA sequencing method based on AFM force spectroscopy (Figure 1). In this approach, four dNTPs (dATP, dTTP, dGTP, and dCTP) are immobilized on separate regions on a glass slide. A DNAP is conjugated to an AFM tip, and the DNAP is allowed to capture a primer-template DNA. The tip then approaches a dNTP spot and measures the interaction between the DNAP and the dNTP. If the dNTP under examination is complementary to the template base that resides in the active site of DNAP, the dNTP will fit into the site to form a ternary complex,²⁵ and a specific rupture event is expected to occur upon tip retraction. If the dNTP is not complementary to the template base, a specific rupture event will not be observed. By the sequential examination of all four dNTP spots, the matching dNTP can be identified (Figure 1a). Then, to enable the next template base to be read, the identified dNTP must be incorporated into the primer. This dNTP can be incorporated by placing the tip into a solution of the dissolved dNTP or preferably by allowing the tip to remain on the spot containing the immobilized dNTP for a certain time (Figure 1b,c). By cycling between specific recognition and incorporation, the sequence of the template DNA can be elucidated.

There were several issues to consider prior to the realization of this sequencing technique. First, dNTPs should be immobilized onto surfaces in an orientation-controlled manner, and immobilized dNTPs should be flexible enough to enable facile interactions with the DNAP/DNA complex. Second, the DNAP used should be able to discriminate matching dNTPs

from nonmatching ones so that the correct base can be read by AFM. Third, the DNAP must lack any undesirable nuclease activity. Fourth, if the direct incorporation of dNTPs from the glass slide spots is the goal, the DNAP should be able to incorporate immobilized dNTPs. Fifth, it is necessary to conjugate the DNAP onto the AFM tip appropriately so that multiple interactions (e.g., interactions between two polymerases and dNTPs) are minimized.

We used γ -phosphate-biotin-labeled dNTPs in our experiments. These dNTPs can be easily immobilized onto a streptavidin surface, and a proper linker was placed between the biotin and phosphate to ensure flexibility (Figure S1). Because γ -phosphate-labeled dNTPs are generally poor substrates for RNAPs and DNAPs,²⁶ we tested several DNAPs for their activities on these dNTP analogs. We selected Terminator γ DNAP because it can incorporate γ -phosphate-biotin dNTPs at the fastest rate at room temperature (Figure S2a). Additionally, Terminator γ DNAP lacks endo- and exonuclease activities, which complicate the sequencing process. Furthermore, we confirmed that the polymerization activity of Terminator γ DNAP was retained even when immobilized on a solid surface (Figure S2b).

Identification of Matching dNTPs. We explored the capability of the DNAP-immobilized AFM tip to specifically recognize matching dNTPs by examining four dNTP spots in a solution containing primer-template DNA (20 nM) (Figure 2). A DNAP-immobilized AFM tip in force-mapping mode was sequentially advanced toward and retracted from four dNTP spots (five cycles per pixel, 10×10 pixels). The approach/retraction speed was kept constant at $0.50 \mu\text{m s}^{-1}$, providing approximately 20 ms contact time. The base of the template DNA in the active site was cytosine, and rupture curves with nonlinear stretching were observed predominantly on the dGTP spot, as clearly shown in the two-dimensional maps (Figure 2a). The number of rupture curves observed for each map was 12 (dATP), 15 (dTTP), 137 (dGTP), and 14 (dCTP). In addition, pixels on which more than one curve was recorded were rare on nonmatching dNTP spots. The rupture force and distance on the dGTP spot were 29 ± 7 pN and 6.4 ± 1.9 nm (mean \pm s.d.), respectively, and the low probability of

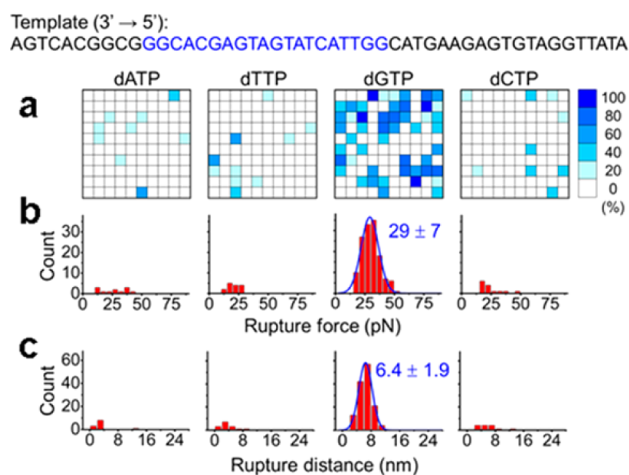


Figure 2. Specific recognition of matching dNTP for a template DNA. The sequence of the template DNA (50-mer) is shown at the top, and the sequence in blue is the primer-binding region (20-mer). The base in the active site is cytosine. (a) Representative force maps on four dNTP spots. The detection probability of specific rupture events on each pixel is indicated by the color scale (10×10 pixels, $1.0 \times 1.0 \mu\text{m}^2$). (b) Rupture force histograms. (c) Rupture distance histograms. (b, c) The most probable rupture force and distance (mean \pm s.d. of Gaussian fit) on the dGTP (matching) spot.

observing curves on the nonmatching spots was evident (Figure 2b,c).

We further investigated the specific recognition of matching dNTPs with the other three template DNAs, which resulted in guanine, thymine, and adenine bases at the active site (Figures S3 and S4). In all cases, we observed the same phenomenon: specific rupture curves were predominantly observed for the matching dNTP.

When we collected the data from five scans (five maps for the matching dNTP and 15 maps for the nonmatching spots), the mean probabilities of observing specific rupture events for matching and nonmatching dNTPs were 22–28% and 1.5–2.8%, respectively (Figures S5 and S6). The most probable rupture forces and distances on the matching dNTPs were 26–32 pN and 5.5–6.3 nm, respectively, and these values are larger than those observed for nonmatching dNTPs. The observed force was within the known range for the protein–ligand pairs, but it was larger than the expected value for single base-pairing.²⁷ Furthermore, a noticeable difference in rupture force was not observed between the matched base pairs (C–G and A–T). This observation likely occurs because the DNAP forms a ternary complex with a target DNA and a dNTP,²⁵ and the rupture force originates from base pair disruption in addition to disruption of the interactions between the phosphate group and the amino acids in the pocket. The distance was reasonable considering the dimensions of the DNAP, the spacer, and

streptavidin, and their stretching without protein unfolding under the rupture force (approximately 30 pN). Thus, in this experimental scheme, the probability of observing a specific curve is an effective criterion with which to determine the base that matches the base bound in the polymerase's active site.

Co-Immobilization of DNAP/DNA for Continuous Sequencing. To read the sequence of a single DNA using this approach, another important parameter is the processivity of the polymerase. Although Terminator γ DNAP is capable of incorporating the dNTP analogs used in this study, its processivity is low (<20 nt).²⁸ With the limited processivity, the DNAP/DNA complex is kinetically labile, and the dissociation of the complex is even faster in the absence of a matching dNTP in the active site.²⁹ Therefore, DNAP will associate with a new primer-template DNA after dissociating from the current DNA template. Such frequent association and dissociation can lead to serious problems.

Our study showed that increasing the concentrations of glycerol and Mg(II) did not sufficiently increase the processivity of Terminator γ DNAP. Employing processivity-enhanced polymerases is an option,^{28,30,31} but a loss of DNA is still a possibility, especially when extended times (approximately 10 min per map) are taken to complete the sequencing.

To address this issue, we covalently immobilized both the primer DNA and the polymerase onto the AFM tip (Figure 3). In this scheme, the released primer-template can be recaptured by DNAP, enabling continuous sequencing. For DNA immobilization, we used a primer DNA with a 5' primary amine label with a 20 thymine spacer. To efficiently immobilize the primer and DNAP adjacent to each other on an AFM tip, we incubated the primer-template DNA and DNAP at equimolar concentration ($1.0 \mu\text{M}$) to form a complex prior to conjugation to the AFM tip. The validity of this approach was confirmed by examining the specific force curves of these tips (Figure S7). We found that 20% of the tips (2 out of 10 tips) worked properly. Possible reasons for the low yield include the following: (1) the orientation of the DNAP was not controlled; therefore, the active site of DNAP might not have been accessible to the surface-conjugated dNTPs; (2) the primer and DNAP were immobilized at a non-optimal position on the AFM tip; and (3) the primer was immobilized at a position that was not adjacent to the DNAP, potentially hindering efficient reassociation. Despite the low yield, this study confirmed that co-immobilization of primer and DNAP enables the use of a distributive polymerase. To improve yields, further optimization of the preparation conditions is needed.

Repeated On-Chip Recognition and In-Solution Incorporation. We performed continuous sequencing with the co-immobilized DNAP/DNA AFM tip in a solution in which the primer-template DNA was not supplemented. For the co-immobilized DNAP/DNA tip, the probabilities of observing specific rupture curves for matching and non-

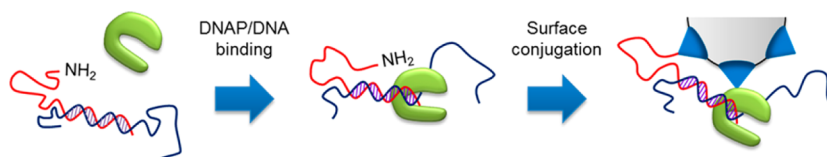


Figure 3. Co-immobilization of a DNAP and a primer on an AFM tip. The primer was labeled with a primary amine at the 5'-end with a T20 spacer for covalent immobilization. A DNAP and a primer-template DNA were first allowed to form a complex. Subsequently, an AFM tip was immersed in a solution containing the complex, resulting in immobilization of the DNAP and primer adjacent to each other.

matching dNTPs were 23–24% and 2.6–3.1%, respectively (Figures S8 and S9). The most probable rupture force was 26–30 pN for the matching dNTPs. The rupture probability and force observed here were similar to values observed for the DNAP-immobilized tip, whereas the rupture distance (4.4–4.6 nm) was shorter and the distance variation among tips was higher for the co-immobilized DNAP/DNA tip. We speculate that the overall reduction and relatively large variation in rupture distance are associated with variations in the polymerase immobilization site on the tip.

For a template DNA with cytosine as the first base, we observed specific rupture events mainly on the dGTP spot (Figure 4). To incorporate dGTP, the AFM tip was detached

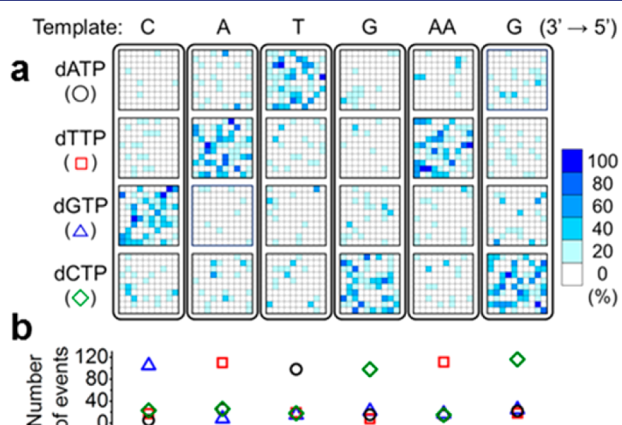


Figure 4. Reading a single DNA sequence by repeating on-chip recognition and in-solution incorporation. (a) The bases of the template DNA in the active site of the DNAP/DNA complex are shown at the tops of the columns. Four maps per column were recorded by successive force-mapping on the four dNTP spots. After the identification of the matching dNTP by comparing detection probability, the AFM tip was immersed in the matching dNTP solution for incorporation. Completion of incorporation was confirmed by the specific recognition of the next base. Consecutive adenines (the fifth and sixth bases) were read as a single adenine due to the simultaneous incorporation of two thymines. (b) Number of specific rupture events observed at each recognition step. The numbers of specific rupture events were noticeably higher for matching dNTPs than for nonmatching dNTPs.

from a tip holder and immersed into a separate chamber filled with a solution of dGTP (1.0 mM) at 25 °C for 5 min. The successful incorporation of dGTP was verified by the disappearance of specific rupture events on the dGTP spot and the increased detection of rupture events on the dTTP spot; thymine was complementary to the next base of the template DNA. Sequential sequencing could be performed for subsequent bases.

Notably, we repeatedly observed the specific rupture force within the entire region of a map. If surface-immobilized dNTP analogs were incorporated into the complementary strand during the measurement, the rupture event should disappear. These data indicate that matching dNTPs were not incorporated into the complementary strand under the current conditions.

Two consecutive adenines (fifth and sixth bases) were read as a single adenine because two thymines were incorporated during a single immersion in the dTTP solution. To avoid this problem, we identified a condition that allows Terminator γ DNAP to only incorporate one dTTP at a time, even when two

sequential adenines are present in the template. Gel electrophoresis showed that one dTTP, but not two, was incorporated by the DNAP in a 10 μ M dTTP solution at 25 °C for 1.0 min. Under these conditions with the co-immobilized DNAP/DNA tip, we could incorporate the first thymine and recognize the second thymine (Figure S10). These results suggest that sequencing a template DNA with homopolymeric regions would be feasible if optimized conditions are used to limit incorporation to single bases.

We failed to read any bases after the seventh base (G) (Figure 4), and the process was commonly terminated after incorporating a few bases (approximately five), as indicated by the disappearance of specific rupture curves at all four dNTP spots. Possible causes of termination are (1) physical damage to the AFM tip (2000 measurements per base); (2) damage or contamination of the DNAP (it took approximately 1 h to read a base and incorporate the matching base); and (3) limited elasticity of the primer conjugated onto the AFM tip. As the primer DNA is extended via dNTP incorporation, the spacer connecting the AFM tip and the primer should be flexible and lengthy to allow the primer to be effectively extended.

To understand the causes of termination, we decreased the potential for tip damage by decreasing the number of measurements per map from 500 to 75 (three measurements per pixel, 5 \times 5 pixels, 1.0 \times 1.0 μ m²) (Figure S11). With this change, the numbers of specific curves on the matching and nonmatching dNTP spots were 15 \pm 2 (20 \pm 2%) and 3 \pm 1 (4 \pm 2%) (mean \pm s.d.), respectively. Under the latter force-mapping condition, we could read up to the 11th base (G) (the adenines in the fifth and sixth position were read as a single adenine), while complementary bases were incorporated using a 1.0 mM dNTP solution for 1.0 min. Because the number of measurements was only 3000, the limited stretching length of the immobilized primer should be the main cause of termination.

We demonstrate that the two-step process followed by AFM can read individual bases at the single-DNA level. The use of an optimized linker for the primer and a microfluidic cell that supplies a recognized dNTP to the AFM probe will make this single DNA sequencing approach more applicable.

On-Chip Incorporation of dNTP. Whereas the use of a microfluidic cell will make the two-step process convenient, direct incorporation of dNTPs immobilized on a surface will render the approach more efficient. To examine DNAP activity on surface-immobilized dNTPs, we investigated the incorporation of streptavidin-bound γ -phosphate-dNTP-biotin by Terminator γ DNAP in solution. Only the dGTP analog was incorporated at a rate of approximately 0.1 nt s⁻¹; the other dNTP analogs were not incorporated within 30 min. The bulky pendant at the γ position likely deterred dNTP incorporation; thus, dGTP was a good candidate with which to test on-chip incorporation.

The incorporation of a nucleotide (phosphodiester bond formation) is preceded by a conformational change in the DNAP.³² Therefore, we employed the force-clamp mode to control the mechanical stress applied to the enzyme upon contact with surface-tethered dNTPs. In force-clamp mode, the distance between the AFM tip and a surface is controlled by force-feedback to keep the applied force constant.¹⁶

After measuring the specific curves at a spot containing tethered dGTP, we brought the AFM tip to a pixel where the specific rupture curves were observed persistently and switched to force-clamp mode (Figure 5a). In this mode, the tip was

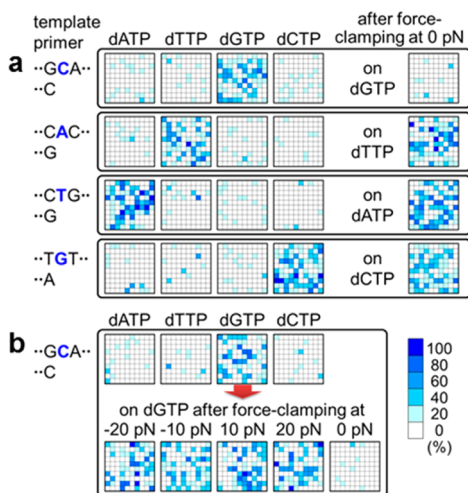


Figure 5. On-chip incorporation of surface-conjugated dGTP. The corresponding sequences of the template and primer DNA are shown to the left of each row. (a) After the identification of the matching dNTP, the AFM tip was brought to a dNTP on the matching dNTP spot and allowed to contact the surface-conjugated dNTP using force-clamping. After force-clamping, the matching dNTP spot was rescanned. When the incorporation was successful (in the case of dGTP (first row)), rupture events on the dGTP spot were rarely observed compared to the prior scanning. When incorporation was not successful (dTTP (second row), dATP (third row), and dCTP (fourth row)), rupture events were persistently observed. (b) Applied-force-dependent incorporation of surface-conjugated dGTP. Incorporation did not occur under compressing (-20 and -10 pN) or stretching (10 and 20 pN) force-clamp conditions, succeeding only at 0 pN.

moved to the contact point and kept in contact with dGTP while the vertical force was maintained at 0 pN for 10 s and then lifted (Figure S12). The clamping process was repeated 10 times (total contact time of 100 s) to allow the DNAP to interact with dGTP at various orientations. After this process, the probability of observing a specific rupture curve was reduced dramatically. Incorporation was confirmed by observing the specific recognition of the next base in the sequence (A). However, the dTTP was not incorporated under these conditions, as the specific recognition of dTTP was persistent. Additionally, no incorporation of dATP or dCTP was observed, as expected. The incorporation of tethered dGTP but no other dNTPs accorded with the facile incorporation of hindered dGTP in the solution phase.

To understand the effect of applied force on the incorporation activity of the tip-attached DNAP, the incorporation of surface-conjugated dGTP was examined under various clamping forces (Figure 5b). Interestingly, incorporation was not observed under compressing conditions (-20 and -10 pN) or stretching conditions (10 and 20 pN). After a compressing or stretching force was applied for 100 s (10 s \times 10 times), specific interaction with dGTP was observed repeatedly. dGTP incorporation was only successful when the applied force was zero; incorporation was confirmed by the disappearance of dGTP recognition and the recognition of dTTP for the next base (A). This force dependence should be taken into consideration when similar approaches are explored and may serve as a useful factor with which to control DNAP reactivity.

DISCUSSION

Here, we established an AFM-based single DNA sequencing method that can be classified as SBS. In conventional SBS platforms, the detection of signals from an incorporated base is followed by the identification of the base from which the signal originated. In contrast, in our approach, the matching base is recognized by observing a specific interaction on a corresponding dNTP spot prior to incorporation. We did not observe any error in the recognition step (substitution error) with the DNAP/DNA tip for at least four independent scans. Although the deletion error occurred for homopolymeric adenines when using a high dTTP concentration, this problem can be avoided by optimizing the incorporation conditions, as demonstrated in our study, or by using dNTP analogs that are tagged with a reversible terminator.² Because the commercially available high-throughput sequencing platforms were reported to have approximately 0.5% insertion/deletion errors and a 0.1% substitution error,³³ and the error from the single read with the single-molecule sequencing technique was reported to be above 10% ,⁶ the high accuracy of our approach is certainly advantageous.

For the co-immobilized DNAP/primer tip, template DNA can be washed out at high temperatures (Therminator γ DNAP is active at 75 °C), and another DNA molecule can be captured for sequencing. Accordingly, DNAs from various samples can be sequenced with a single tip as long as the tip remains mechanically intact. Although a co-immobilization scheme solved the processivity issue, this scheme led to limited read length and a low yield of functional tips. For longer read lengths, the length of the spacer and primer should be judiciously designed. Because the tip remained intact for up to 1.2×10^4 measurements, reduced numbers of measurements at each pixel (as in Figure S11) are expected to allow read lengths up to 40 bases if an appropriate linker for the primer is used. Ultimately, the use of a DNAP that has been modified for exceptional processivity and oriented immobilization will simplify tip preparation.²⁸

To reduce the analysis time, force-mapping parameters such as speed and the number of measurements and pixels can be optimized. In addition, fast AFM machines such as TREC and high-speed AFM can be employed to reduce the scan time.^{34–36} An additional advantage is decreased tip damage due to reduced physical contact. The use of a microfluidic cell that supplies a recognized dNTP to the AFM probe will eliminate the laborious steps of removing the probe from the AFM, dipping it into the solution and returning it to the instrument. Additionally, on-chip incorporation would allow for more efficient analysis as well as miniaturization. To achieve on-chip incorporation, nucleotides with tetra- or penta-phosphates^{26,37} and activity-enhanced DNAP should be examined; however, these modifications may result in the incorporation of the matching dNTP during the contact time of the force-mapping. Controlling the contact time and applied force in the force-mapping may prevent unwanted dNTP incorporation.

In addition, we found that Therminator γ DNAP reactivity was impaired under mechanical stress. However, in some cases, enhanced enzymatic activity has been reported when a mechanical force was applied.³⁸ Thus, it might be possible to develop a DNAP that has enhanced activity at a specific force range for controlled dNTP incorporation on chips.

This method is expected to be suitable for targeted gene sequencing at the single-DNA level without the need for

labeling, if the tip preparation method, force-mapping parameters, and incorporation condition are optimized for the enhanced yield, speed, and read length. Furthermore, direct sequencing of RNA may be possible if reverse transcriptase is used in place of DNAP.

■ EXPERIMENTAL SECTION

Oligonucleotides and dNTP Analogs. The oligonucleotides that were used as primers and templates were custom synthesized (Bioneer, Korea) (Table S1). The melting temperature of the primer/DNA was reported as 49 °C by the manufacturer. We designed a template DNA (50-mer) to have a common primer-binding region (20-mer) 10 bp away from the 3' end.

Four dNTP analogs (γ -[6-aminohexyl]-dNTP-biotin) were custom synthesized (Jena Bioscience, purity >95% (HPLC)) (Figure S1).

Preparation of dNTP-Immobilized Slides. Four spots on an NSB9 amine glass slide (NSB POSTECH Inc.) were reacted with 34 mM NHS-PEG4-biotin (Thermo Scientific) in PBS for 2.0 h. The biotinylated slide was washed with PBST, rinsed with deionized water, and dried under vacuum (30–40 mTorr). We incubated a streptavidin solution (Sigma-Aldrich) (1.0 mM in PBS) on the biotinylated spots at room temperature for 1.0 h. We washed away any excess streptavidin with PBST and rinsed the slide with deionized water. We spotted each of four γ -phosphate biotin-labeled dNTPs (500 μ M in PBS) onto separate regions of the streptavidin surface, and the dNTP analogs were immobilized at room temperature for 1.0 h. Unbound dNTP analogs were washed away with PBST, and the slide was rinsed with deionized water, spin-dried (1000g, 100 s), and stored in PBS at 4 °C until its usage.

Immobilization of the DNAP or the DNAP/Primer on AFM Tips. We coated AFM tips (DPN Probe Type B, NanoInk) with 27-acid dendrons as previously described.³⁹ Briefly, silicon nitride probes were oxidized in 10% nitric acid solution at 80 °C for 20 min. For silanization, the probes were placed in a toluene solution containing *N*-(3-(triethoxysilyl)propyl)-*O*-poly(ethylene oxide) urethane (Gelest) (1% (v/v)) for 4 h. The silanized probes were immersed in a methylene chloride solution containing 27-acid dendron (dissolved in a minimal amount of dimethylformamide, final conc. 1.0 mM), 1,3-dicyclohexylcarbodiimide (27 mM), and 4-dimethylaminopyridine (0.90 mM) for 12 h. Subsequently, the protecting groups at the apexes of immobilized dendrons were removed with trifluoroacetic acid, exposing amine groups. Then, the probes were reacted with disuccinimidyl carbonate (25 mM in acetonitrile) to generate *N*-hydroxysuccinimide groups at the apexes of the dendrons.

We dialyzed Terminator γ DNAP against sodium bicarbonate buffer (25 mM Na₂HCO₃, 5 mM MgCl₂, pH 8.5) using a D-tube Dialyzer Mini (MWCO 6–8 kDa, Novagen). We then immersed NHS-modified AFM tips in the dialyzed DNAP solution (2.0 μ M) at room temperature for 2.0 h and washed them with PBST followed by Terminator γ DNAP reaction buffer (20 mM Tris-HCl, 50 mM KCl, 5.0 mM MgSO₄, 0.02% IGEPAL CA-630 (v/v), pH 9.2).

To co-immobilize DNAP and primer on an AFM tip, we formed a DNAP/DNA complex prior to the conjugation on the tip. First, we added template and 5' amine-labeled primer DNA (each 10 μ M) to sodium bicarbonate buffer, incubated the solution at 95 °C for 3.0 min, and cooled the solution slowly to room temperature. We mixed the annealed dsDNA and the dialyzed polymerase solution (final concentration 1.0 μ M each) and incubated the mixture at room temperature for 1.0 h to form the complex. Then, NHS-modified AFM tips were immersed in the solution at room temperature for 2.0 h and washed as above. The prepared AFM tips were used immediately.

AFM Force Spectroscopy and Data Analysis. AFM force-mapping and force-clamping were carried out using a ForceRobot 300 (JPK Instruments) equipped with an antivibration table (Halcyonics Micro 40, Accurion) and an isolation chamber (Herzan). After sample mounting, we waited 30 min for system stabilization and temperature equilibration. The AFM cantilever (DPN Probe Type B-1b, NanoInk) was calibrated with a built-in program based on the thermal fluctuation method (spring constant 0.011–0.022 N·m⁻¹).

With the DNAP-immobilized tip, we performed force-mapping in Terminator γ DNAP reaction buffer containing primer-template DNA (20 nM). We recorded force maps (10 × 10 pixels, 1.0 × 1.0 μ m²) on the four dNTP spots sequentially by collecting five force–distance curves on each pixel with a constant approach and retraction speed (0.50 μ m s⁻¹). The maximum applied force was set as 50–100 pN to minimize mechanical damage to the AFM tip. The slope of each force–distance curve was analyzed, and the curves that showed the bond rupture with a nonlinear stretching profile were used for further analysis. The value of the peak for rupture was taken to measure the rupture force value. The most probable values on the force and distance histograms were calculated by Gaussian fitting (OriginPro 8).

With the co-immobilized DNAP/DNA tip, we performed force-mapping in Terminator γ DNAP reaction buffer that was not supplemented with primer-template DNA. The force-mapping parameters were same as the case of the DNAP-immobilized tip if not otherwise stated.

In-Solution Incorporation of Matching dNTPs. To incorporate the identified dNTP, we detached the cantilever from the AFM cantilever holder and immersed it in polymerase reaction buffer containing the matching dNTP (1.0 mM) at 25 °C for 5.0 min (if not stated otherwise). Then, the cantilever was washed thoroughly with reaction buffer without dNTP. We returned the cantilever back to the AFM setup and waited 15 min for system stabilization prior to subsequent force-mapping.

On-Chip Incorporation of Matching dNTPs. For the direct incorporation of the identified dNTP from the chip surface, we scanned the matching dNTP spot to find a pixel on which specific rupture curves were consistently observed. Bringing the DNAP/DNA-immobilized tip to the pixel ensured the accessibility of the matching dNTP to the DNAP active site. Then, we switched to force-clamp mode. In this mode, the AFM tip was programmed to approach the spot, retract until the repulsive force decreased to zero (0 pN), and maintain a zero force for 10 s. The approach and retraction speed was kept at 0.50 μ m s⁻¹, and the data sampling rate of 1000 Hz was used. We repeated the force-clamping process 10 times at a fixed lateral position to increase the probability of incorporating a surface-conjugated dNTP.

To study the effect of the applied force on the incorporation activity of Terminator γ DNAP for surface-immobilized dGTP, we attempted on-chip incorporation under various clamping forces (–20, –10, 10, 20, and 0 pN (sequentially); negative and positive forces indicate compressing and stretching forces, respectively). After dGTP recognition, we performed force-clamping at –20 pN as described above. Subsequently, we recorded a force map on the dGTP spot to verify the success of incorporation. Upon persistent observation of rupture events on the spot, we repeated this step with different clamping forces.

■ ASSOCIATED CONTENT

Supporting Information

Additional experimental procedures, figures, and a table (Figure S1–S12, Table S1). This material is available free of charge via the Internet at <http://pubs.acs.org>.

■ AUTHOR INFORMATION

Corresponding Author

jwpark@postech.ac.kr

Notes

The authors declare the following competing financial interest(s): A patent application has been filed by LG Electronics Inc. under international publication number WO 2013/065881 A1: Apparatus and method for determining sequences of nucleic acids using atomic force microscope. A patent application has been filed by LG Electronics Inc. and Pohang University of Science and Technology under Korean

application number 10-2013-0158969: Method for sequencing nucleic acids using atomic force microscope.

ACKNOWLEDGMENTS

This work was supported by grants from LG Electronics Inc. and the Brain Korea 21 plus program.

REFERENCES

- (1) Manolio, T. A. *N. Engl. J. Med.* **2010**, *363*, 166.
- (2) Metzker, M. L. *Nat. Rev. Genet.* **2010**, *11*, 31.
- (3) Pareek, C. S.; Smoczynski, R.; Tretyn, A. *J. Appl. Genet.* **2011**, *52*, 413.
- (4) Rothberg, J. M.; Hinz, W.; Rearick, T. M.; Schultz, J.; Mileski, W.; Davey, M.; Leamon, J. H.; Johnson, K.; Milgrew, M. J.; Edwards, M.; Hoon, J.; Simons, J. F.; Marran, D.; Myers, J. W.; Davidson, J. F.; Branting, A.; Nobile, J. R.; Puc, B. P.; Light, D.; Clark, T. A.; Huber, M.; Branciforte, J. T.; Stoner, I. B.; Cawley, S. E.; Lyons, M.; Fu, Y.; Homer, N.; Sedova, M.; Miao, X.; Reed, B.; Sabina, J.; Feierstein, E.; Schorn, M.; Alanjary, M.; Dimalanta, E.; Dressman, D.; Kasinskas, R.; Sokolsky, T.; Fidanza, J. A.; Namsaraev, E.; McKernan, K. J.; Williams, A.; Roth, G. T.; Bustillo, J. *Nature* **2011**, *475*, 348.
- (5) Xu, M.; Fujita, D.; Hanagata, N. *Small* **2009**, *5*, 2638.
- (6) Eid, J.; Fehr, A.; Gray, J.; Luong, K.; Lyle, J.; Otto, G.; Peluso, P.; Rank, D.; Baybayan, P.; Bettman, B.; Bibillo, A.; Bjornson, K.; Chaudhuri, B.; Christians, F.; Cicero, R.; Clark, S.; Dalal, R.; Dewinter, A.; Dixon, J.; Foquet, M.; Gaertner, A.; Hardenbol, P.; Heiner, C.; Hester, K.; Holden, D.; Kearns, G.; Kong, X.; Kuse, R.; Lacroix, Y.; Lin, S.; Lundquist, P.; Ma, C.; Marks, P.; Maxham, M.; Murphy, D.; Park, I.; Pham, T.; Phillips, M.; Roy, J.; Sebra, R.; Shen, G.; Sorenson, J.; Tomaney, A.; Travers, K.; Trulson, M.; Vieceli, J.; Wegener, J.; Wu, D.; Yang, A.; Zaccarin, D.; Zhao, P.; Zhong, F.; Korlach, J.; Turner, S. *Science* **2009**, *323*, 133.
- (7) Chen, Y. S.; Lee, C. H.; Hung, M. Y.; Pan, H. A.; Chiou, J. C.; Huang, G. S. *Nat. Nanotechnol.* **2013**, *8*, 452.
- (8) Venkatesan, B. M.; Bashir, R. *Nat. Nanotechnol.* **2011**, *6*, 615.
- (9) Cracknell, J. A.; Japrun, D.; Bayley, H. *Nano Lett.* **2013**, *13*, 2500.
- (10) Tanaka, H.; Kawai, T. *Nat. Nanotechnol.* **2009**, *4*, 518.
- (11) Huang, S.; He, J.; Chang, S.; Zhang, P.; Liang, F.; Li, S.; Tuchband, M.; Fuhrmann, A.; Ros, R.; Lindsay, S. *Nat. Nanotechnol.* **2010**, *5*, 868.
- (12) Greenleaf, W. J.; Block, S. M. *Science* **2006**, *313*, 801.
- (13) Ding, F.; Manosas, M.; Spiering, M. M.; Benkovic, S. J.; Bensimon, D.; Allemand, J. F.; Croquette, V. *Nat. Methods* **2012**, *9*, 367.
- (14) Hinterdorfer, P.; Dufrêne, Y. F. *Nat. Methods* **2006**, *3*, 347.
- (15) Muller, D. J.; Dufrêne, Y. F. *Nat. Nanotechnol.* **2008**, *3*, 261.
- (16) Fernandez, J. M.; Li, H. *Science* **2004**, *303*, 1674.
- (17) Kufer, S. K.; Puchner, E. M.; Gump, H.; Liedl, T.; Gaub, H. E. *Science* **2008**, *319*, 594.
- (18) Husale, S.; Persson, H. H.; Sahin, O. *Nature* **2009**, *462*, 1075.
- (19) Kim, J. S.; Jung, Y. J.; Park, J. W.; Shaller, A. D.; Wan, W.; Li, A. D. Q. *Adv. Mater.* **2009**, *21*, 786.
- (20) Kim, E. S.; Kim, J. S.; Lee, Y.; Choi, K. Y.; Park, J. W. *ACS Nano* **2012**, *6*, 6108.
- (21) Hansma, H.; Weisenhorn, A.; Gould, S.; Sinsheimer, R.; Gaub, H.; Stucky, G.; Zarella, C.; Hansma, P. J. *Vac. Sci. Technol. B* **1991**, *9*, 1282.
- (22) Woolley, A. T.; Guillemette, C.; Li Cheung, C.; Housman, D. E.; Lieber, C. M. *Nat. Biotechnol.* **2000**, *18*, 760.
- (23) Qamar, S.; Williams, P. M.; Lindsay, S. M. *Biophys. J.* **2008**, *94*, 1233.
- (24) Bailo, E.; Deckert, V. *Angew. Chem., Int. Ed.* **2008**, *47*, 1658.
- (25) Rodriguez, A. C.; Park, H. W.; Mao, C.; Beese, L. S. *J. Mol. Biol.* **2000**, *299*, 447.
- (26) Kumar, S.; Sood, A.; Wegener, J.; Finn, P. J.; Nampalli, S.; Nelson, J. R.; Sekher, A.; Mitsis, P.; Macklin, J.; Fuller, C. W. *Nucleosides, Nucleotides Nucleic Acids* **2005**, *24*, 401.
- (27) Lee, C. K.; Wang, Y. M.; Huang, L. S.; Lin, S. *Micron* **2007**, *38*, 446.
- (28) Williams, J. G.; Steffens, D. L.; Anderson, J. P.; Urlacher, T. M.; Lamb, D. T.; Grone, D. L.; Egelhoff, J. C. *Nucleic Acids Res.* **2008**, *36*, e121.
- (29) Markiewicz, R. P.; Vrtis, K. B.; Rueda, D.; Romano, L. J. *Nucleic Acids Res.* **2012**, *40*, 7975.
- (30) Wang, Y.; Prosen, D. E.; Mei, L.; Sullivan, J. C.; Finney, M.; Vander Horn, P. B. *Nucleic Acids Res.* **2004**, *32*, 1197.
- (31) Davidson, J. F.; Fox, R.; Harris, D. D.; Lyons-Abbott, S.; Loeb, L. A. *Nucleic Acids Res.* **2003**, *31*, 4702.
- (32) Berdis, A. J. *Chem. Rev.* **2009**, *109*, 2862.
- (33) Jünemann, S.; Sedlazeck, F. J.; Prior, K.; Albersmeier, A.; John, U.; Kalinowski, J.; Mellmann, A.; Goesmann, A.; von Haeseler, A.; Stoye, J.; Harmsen, D. *Nat. Biotechnol.* **2013**, *31*, 294.
- (34) Zhu, R.; Rupprecht, A.; Ebner, A.; Haselgrübler, T.; Gruber, H. J.; Hinterdorfer, P.; Pohl, E. E. *J. Am. Chem. Soc.* **2013**, *135*, 3640.
- (35) Ando, T.; Kodera, N.; Takai, E.; Maruyama, D.; Saito, K.; Toda, A. *Proc. Natl. Acad. Sci. U.S.A.* **2001**, *98*, 12468.
- (36) Rico, F.; Gonzalez, L.; Casuso, L.; Puig-Vidal, M.; Scheuring, S. *Science* **2013**, *342*, 741.
- (37) Sood, A.; Kumar, S.; Nampalli, S.; Nelson, J. R.; Macklin, J.; Fuller, C. W. *J. Am. Chem. Soc.* **2005**, *127*, 2394.
- (38) Gump, H.; Puchner, E. M.; Zimmermann, J. L.; Gerland, U.; Gaub, H. E.; Blank, K. *Nano Lett.* **2009**, *9*, 3290.
- (39) Jung, Y. J.; Albrecht, J. A.; Kwak, J. W.; Park, J. W. *Nucleic Acids Res.* **2012**, *40*, 11728.